# Fission Yeast Mutants Affecting Telomere Clustering and Meiosis-Specific Spindle Pole Body Integrity

**Ye Jin, Satoru Uzawa and W. Z. Cande**[1]

*Department of Molecular and Cell Biology, University of California, Berkeley, California 94732*

Manuscript received April 2, 2001
Accepted for publication December 10, 2001

ABSTRACT

In meiotic prophase of many eukaryotic organisms, telomeres attach to the nuclear envelope and form a polarized configuration called the bouquet. Bouquet formation is hypothesized to facilitate homologous chromosome pairing. In fission yeast, bouquet formation and telomere clustering occurs in karyogamy and persists throughout the horsetail stage. Here we report the isolation and characterization of six mutants from our screen for meiotic mutants. These mutants show defective telomere clustering as demonstrated by mislocalization of Swi6::GFP, a heterochromatin-binding protein, and Taz1p::GFP, a telomere-specific protein. These mutants define four complementation groups and are named *dot1* to *dot4*—*d*efective *o*rganization of *t*elomeres. *dot3* and *dot4* are allelic to *mat1-Mm* and *mei4*, respectively. Immunolocalization of Sad1, a protein associated with the spindle pole body (SPB), in *dot* mutants showed an elevated frequency of multiple Sad1-nuclei signals relative to wild type. Many of these Sad1 foci were colocalized with Taz1::GFP. Impaired SPB structure and function were further demonstrated by failure of spore wall formation in *dot1*, by multiple Pcp1::GFP signals (an SPB component) in *dot2*, and by abnormal microtubule organizations during meiosis in *dot* mutants. The coincidence of impaired SPB functions with defective telomere clustering suggests a link between the SPB and the telomere cluster.

ALL sexually reproducing organisms undergo meiosis to produce haploid gametes. In meiosis, a single diploid mother cell gives rise to four haploid gametes by two consecutive cell divisions following one round of DNA replication. Meiosis consists of both reductional (meiosis I) and equational (meiosis II) divisions and is dominated by the prophase of meiosis I, which can be further divided into five sequential stages—leptotene, zygotene, pachytene, diplotene, and diakinesis according to morphological changes of chromosomes. Many chromatin reorganization events essential for successful completion of meiosis occur in meiotic prophase. These events happen sequentially and the occurrence of each event is, more or less, dependent on the previous one. Disruption of some events, such as impaired homologous chromosome pairing and reduction of chromosome crossing over, leads to defective meiotic spindle assembly and chromosome nondisjunction at anaphase (reviewed in Zickler and Kleckner 1998).

One commonly reported event in the chromatin spatial reorganization during meiotic prophase is telomere clustering or bouquet formation. Bouquet formation refers to the process in which chromosome ends become attached to the inner membrane of the nuclear envelope and move into a polarized configuration within the nucleus (John 1990; Loidl 1990; Scherthan *et al.* 1994; Dernburg *et al.* 1995). Bouquet formation is highly conserved and found in most eukaryotic organisms including yeast and humans. The bouquet forms at late leptotene and early zygotene and is coincident with chromosome pairing. Because of the temporal relationship of bouquet formation and homologous chromosome pairing, it has been proposed that the function of the bouquet is to facilitate pairing by aligning homolog ends and thus bringing them into close proximity (Bass *et al.* 1997; reviewed in Zickler and Kleckner 1998). Disruption of the bouquet in mutants from a variety of organisms, such as *dsy498** in maize, *ndj1* in budding yeast, and *taz1* and *kms1* in fission yeast, results in the severe disruption of gametogenesis and sporulation (Cooper *et al.* 1998; Niwa *et al.* 2000; Trelles-Sticken *et al.* 2000; I. Golubovskaya and W. Z. Cande, personal communication). Although a conserved importance for the bouquet is evident in meiosis, little is known about the mechanism of its formation and maintenance, especially at a molecular level. Thus, one of our major efforts is to understand bouquet formation.

Fission yeast is an excellent organism for the study of bouquet formation. First, it provides a genetically amenable system with a nearly completely sequenced genome. Second, compared to the transient bouquet stage in other organisms, telomere clustering in fission yeast is conspicuous and persists throughout meiotic prophase. Third, cytological features of nuclear architecture and cytoskeleton reorganization during meiotic prophase in fission yeast have been well characterized (Robinow 1977; Robinow and Hyams 1989; Bähler *et al.* 1993;

[1]*Corresponding author:* 341 Life Science Addition, Department of Molecular and Cell Biology, University of California, Berkeley, CA 94732. E-mail: zcande@uclink4.Berkeley.edu

Chikashige *et al.* 1994, 1997; Hagan and Yanagida 1995; Svoboda *et al.* 1995; Ding *et al.* 1998), as illustrated in Figure 1A. In vegetatively growing haploid cells of fission yeast, interphase chromosomes form a Rabl configuration in which the centromere cluster is attached to the SPB (spindle pole body) and telomeres occupy the other side of the nucleus due to the poleward movement of centromeres at the previous anaphase. Upon nitrogen starvation and pheromone stimulation, a global chromosome rearrangement occurs in two steps in the cells committed to meiosis. First, telomeres cluster and attach to the SPB. Second, once cytoplasmic fusion occurs between the mating haploid cells, centromeres are released from the SPB, while telomeres remain associated. Following these chromosomal rearrangements, nuclear fusion initiates from the two adjacent SPBs and extends to the rest of the nuclei. After nuclear fusion, the zygotic nucleus undergoes oscillatory movements along astral microtubule tracks with the SPB and telomeres cluster at the leading edge of the moving nucleus. During this dynamic horsetail stage, the DNA is replicated, homologous chromosomes pair, and recombination takes place.

Along with the global remodeling of nuclear architecture, the microtubule cytoskeleton also undergoes reorganization. In vegetatively growing interphase cells, cytoplasmic microtubule bundles nucleate from multiple sites on the nuclear envelope and extend longitudinally along the cell. In meiotic cells, immediately after cytoplasmic fusion, microtubules are nucleated exclusively from SPBs. A typical X-shaped configuration is present during nuclear fusion, followed by formation of a long curved microtubule array that extends from the cell ends and provides the tracks for nuclear horsetail movement. Microtubule depolymerizing drugs and a dynein heavy chain mutation (*dhc*) abrogate the horsetail movement without affecting telomere clustering (Svoboda *et al.* 1995; Yamamoto *et al.* 1999).

The molecular mechanisms responsible for telomere clustering and attachment to the SPB are largely unknown. However, some clues have emerged from studies of mutants displaying defects in telomere clustering. Two classes of proteins required for telomere clustering in *Schizosaccharomyces pombe* have been identified so far: proteins necessary for telomere maintenance (Lot2 and Taz1/Lot3) and proteins important for SPB integrity during meiosis (Kms1; Shimanuki *et al.* 1997; Cooper *et al.* 1998; Nimmo *et al.* 1998). $lot2^+$ and $taz1^+$ genes encode telomere proteins that are essential for maintaining normal telomere length. In *lot2* and *taz1* mutants, attachment of telomeres to the SPB is disrupted and telomeres become dispersed within the nucleus. Horsetail movement is impaired and a high frequency of chromosome missegregation occurs. Although most zygotes of *lot2* and *taz1* mutants still can sporulate, spore viability and recombination rates are compromised. $kms1^+$ encodes a meiosis-specific SPB-associated component and, so far, *kms*1 is the only reported SPB mutant sharing a similar phenotype with *lot2* and *taz1* mutants in bouquet formation. In *kms1* mutant cells, the localization of another SPB associated component, Sad1, is severely disrupted as indicated by multiple Sad1-immunostaining foci within nuclei. Although Kms1 physically interacts with Sad1, the functional relationship between Sad1 and Kms1 is not known (Niwa *et al.* 2000).

In this study, we report the isolation and characterization of six meiotic bouquet mutants in *S. pombe*. These mutants demonstrate different levels of disruption in telomere clustering and telomere detachment from the SPB. Many of these dispersed Taz1 signals are colocalized with Sad1, a marker for SPB integrity. We found other defects related to impaired SPB structure and functions. On the basis of our observations, we propose that the defective telomere clustering in these mutants is correlated with impaired meiosis-specific SPB functions. We also found that *dot3* and *dot4* are alleles of *mat1-Mm* and *mei4*, respectively, which indicates that, in addition to telomere and SPB components, transcription factors are also involved in telomere clustering and maintenance of the cluster during horsetail stage.

## MATERIALS AND METHODS

***S. pombe* strains, media, and sporulation conditions:** Table 1 lists the strains used in this study. $swi6^+$*::GFP dot* mutants were obtained by transformation with plasmid pREP41 $swi6^+$*::GFP* $leu2^+$ (Pidoux *et al.* 2000). $taz1^+$*::GFP* (J. Cooper, University of Colorado, Boulder, CO) and $pcp1^+$*::GFP* (T. Davis, University of Washington, Seattle) *dot* mutant strains were constructed by genetic crosses, random sporulation, and selection on rich medium YES plates with 100 μg/ml G418. Both $taz1^+$*::GFP* and $pcp1^+$*::GFP* fusion genes are integrated into the endogenous genome locus as a single copy. Complete medium YES or YPD was used for routine culture and strain maintenance (Gutz *et al.* 1974; Moreno *et al.* 1991). For observation of mating and meiosis, minimal medium MSA or Edinburgh minimal medium (EMM2) plates with appropriate supplements were routinely used (Moreno *et al.* 1991; Egel *et al.* 1994). For sporulation, malt extract (ME) or SPA plates were used. All yeast cells were grown at 25° unless indicated. To obtain meiotic cultures, single colonies were grown in YES overnight at 30° to stationary phase. Cells were then inoculated with 1:100 dilution to EMM2 with supplements and grown overnight with shaking until the cell density reached $2 \times 10^6$ to $2 \times 10^7$ cells/ml. Cells were collected by centrifugation, washed with water, resuspended in three volumes of the pellet size in SPA medium, and spread onto SPA plates. Under these conditions, the first zygote appeared ~6 hr after plating.

**General *S. pombe* genetic and molecular biology techniques:** Standard genetic and molecular biology techniques were used according to Moreno *et al.* (1991) and Alfa *et al.* (1993). For plasmid transformation, the lithium acetate method was used. pREP41 $swi6^+$*::GFP* $leu2^+$ plasmids were cut with *Mlu*I at the unique *ars* site and transformed into selected $h^{90}$ meiotic mutants. $Leu^+$ transformants were selected on EMM2. Stable transformants with DNA inserted presumably into the *ars* site of pREP41 were selected by passing transformants on YES plates for several generations.

**Isolation of sporulation-defective meiotic mutants:** WN03 ($h^{90}$ *leu1-32*) culture was mutagenized with *N*-methyl-*N*′-nitro-*N*-nitrosoguanidine (MNNG) at a concentration of 100 μg/

**TABLE 1**

***S. pombe* strains used in this study**

| Strain | Genotype | Source or reference |
|---|---|---|
| WN03 | *h$^{90}$ leu 1-32* | O. Niwa |
| 972L | *h$^{-}$* | O. Niwa |
| YJ101 | *h$^{90}$ leu1-32 dot1-182* | MNNG of WN03 |
| YJ102 | *h$^{90}$ leu 1-32 dot2-439* | MNNG of WN03 |
| YJ103 | *h$^{90}$ leu 1-32 mat1-Mm143* | MNNG of WN03 |
| YJ104 | *h$^{90}$ leu 1-32 mei4-512* | MNNG of WN03 |
| YJ105 | *h$^{90}$ leu 1-32 mei4-550* | MNNG of WN03 |
| YJ106 | *h$^{90}$ leu 1-32 mei4-636* | MNNG of WN03 |
| ZCH46 | *h$^{+}$ leu 1-32 his2-?* | This lab |
| ZCP01 | *h$^{90}$ leu1-32 swi6$^{+}$::GFP leu2 ade6-M210* | This lab |
| 783C3 | *h$^{90}$ ade6-M216 taz1$^{+}$::GFP kanR* | J. Cooper |
| FYC26 | *h$^{+}$ mei2-16 ade6-M216* | Bresch *et al.* (1968) |
| YJ1011 | *h$^{90}$ leu1-32 dot1-182 swi6$^{+}$::GFP leu2$^{+}$* | YJ101 + p*swi6$^{+}$::GFP leu2$^{+}$* |
| YJ1021 | *h$^{90}$ leu 1-32 dot2-439 swi6$^{+}$::GFP leu2$^{+}$* | YJ102 + p*swi6$^{+}$::GFP leu2$^{+}$* |
| YJ1031 | *h$^{90}$ leu 1-32 mat1-Mm143 swi6$^{+}$::GFP leu2$^{+}$* | YJ103 + p*swi6$^{+}$::GFP leu2$^{+}$* |
| YJ1041 | *h$^{90}$ leu1-32 mei4-512 swi6$^{+}$::GFP leu2$^{+}$* | YJ104 + p*swi6$^{+}$::GFP leu2$^{+}$* |
| YJ1051 | *h$^{90}$ leu1-32 mei4-550 swi6$^{+}$::GFP leu2$^{+}$* | YJ105 + p*swi6$^{+}$::GFP leu2$^{+}$* |
| YJ1061 | *h$^{90}$ leu1-32 mei4-636 swi6$^{+}$::GFP leu2$^{+}$* | YJ106 + p*swi6$^{+}$::GFP leu2* |
| 783C4 | *h$^{-}$ taz1$^{+}$::GFP kan$^{R}$ ade6-M216* | 783C3 × 972L |
| YJ1012 | *h$^{90}$ leu 1-32 dot1-182 taz1$^{+}$::GFP kan$^{R}$* | YJ101 × 783C4 |
| YJ1022 | *h$^{90}$ leu 1-32 dot2-439 taz1$^{+}$::GFP kan$^{R}$* | YJ102 × 783C4 |
| YJ1032 | *h$^{90}$ leu 1-32 mat1-Mm143 taz1$^{+}$::GFP kan$^{R}$* | YJ103 × 783C4 |
| YJ1042 | *h$^{90}$ leu 1-32 mei4-512 taz1$^{+}$::GFP kan$^{R}$* | YJ104 × 783C4 |
| YJ1052 | *h$^{90}$ leu 1-32 mei4-550 taz1$^{+}$::GFP kan$^{R}$* | YJ105 × 783C4 |
| YJ1062 | *h$^{90}$ leu 1-32 mei4-636 taz1$^{+}$::GFP kan$^{R}$* | YJ106 × 783C4 |
| YJ1053 | *h$^{+}$ mei4-550 his2-?* | YJ105 × ZCH46 |
| YJ1063 | *h$^{-}$ mei4-636 leu1-32* | YJ106 × ZCH46 |
| YJ1043 | *h$^{+}$ mei4-512 his2-?* | YJ104 × ZCH46 |
| YJ1013 | *h$^{+}$ dot 1-182 his2-?* | YJ101 × ZCH46 |
| YJ1054 | *h$^{-}$ mei4-550 leu1-32* | YJ105 × ZCH46 |
| YJ1044 | *h$^{-}$ mei4-512 leu 1-32* | YJ104 × ZCH46 |
| YJ1023 | *h$^{-}$ dot2-439 leu1-32* | YJ102 × ZCH46 |
| MB126 | *h$^{90}$ ura4-D18 kms1::ura4$^{+}$* | Shimanuki *et al.* (1997) |
| Y7163 | *h$^{-}$ leu1-32 ura4 ade6 tht1::ura4$^{+}$* | Tange *et al.* (1998) |
| HM123 | *h$^{-}$ leu1-32* | O. Niwa |
| YJ1024 | *h$^{+}$ dot2-439 his2-?* | YJ102 × ZCH46 |
| MP5 | *h$^{-}$ ade6-210 leu1-32 ura4 Pcp1::GFP G418$^{R}$* | T. Davis |
| YJMB1261 | *h$^{-}$ ura4-D18 kms1::ura4$^{+}$* | MB126 × 972L |
| YJMP51 | *h$^{90}$ ade6-210 leu1-32 ura4-D18 Pcp1$^{+}$::GFP G418$^{R}$* | MP5 × 972L |
| YJ1035 | *h$^{90}$ leu1-32 dot2-439 Pcp1$^{+}$::GFP G418$^{R}$* | YJ102 × MP5 |
| EG319 | *Pm-B102 his7 swi2-3 ade6-M210* | Bresch *et al.* (1968) |
| EG367 | *h$^{90}$ Pm$^{-}$/M Pm$^{-}$ M his2 swi2-3 ade6-m210* | R. Egel |
| YJAB44 | *h$^{-}$ leu1-32 mei4::ura4$^{+}$ ade6-210 pat1-114* | This lab |
| EG370 | *Mm-B406 his2 swi2-3 ade6-M210* | Egel and Gutz (1981) |

ml according to the method used by Uemura and Yanagida (1984). Mutagenized cells were grown on rich medium YPD plates at room temperature (23°–25°). The survival rate after the MNNG treatment was 12%. After colonies appeared, replicas were made on sporulation medium ME plates to allow meiosis and sporulation. To examine the completion of meiosis and sporulation, colonies were exposed to iodine vapor to stain spores. Iodine-staining negative colonies were defective in the above processes and were examined under a phase contrast microscope for cell morphology. Colonies with spores were rejected. Colonies without appearance of any zygotes were grouped as sterile and not further investigated. The remaining sporulation-defective mutants were fixed and stained with 1 μg/ml 4′,6-diamidino-2-phenylindole (DAPI) to determine the nuclear morphology and the arrested stage in meiosis. Mutants showing four evenly sized and spaced nuclei in the zygotes were rejected as *spo$^{-}$* mutants. All isolated meiotic mutants were backcrossed to wild type at least three times.

**Complementation test, linkage analysis, and spore viability assay:** Complementation tests were performed by mixing two strains and spotting on SPA medium. After 2–3 days incubation at 25°, plates were subjected to iodine staining and microscopic examination to determine whether spores were formed. If the plate showed dark brown cultures and the frequency of four-spore asci was equivalent to that of the wild-type *h$^{90}$* cells, complementation was judged to have occurred between the two mating strains. Otherwise, complementation was considered negative. The possible allelism between mutants was fur-

ther confirmed by the failure of azygotic meiosis in a heterozygous diploid, which is the absence of spore formation. Linkage analyses were done by random spore analysis (Moreno *et al.* 1991). At least 100 colonies from each cross were examined for linkage. To quantify the sporulation and assess the viable spore yield of *dot* mutants, 0.5 ml of vegetatively growing cells in log phase ($\sim 1 \times 10^7$ cells/ml) was spotted on an SPA plate to induce meiosis. After 3 days, the cell cultures were collected, treated with β-glucuronidase, and plated on YES plates. The viable spore yield is the number of colonies formed on YES plates divided by the number of cells put on the SPA plates.

**Immunofluorescence microscopy:** Immunostaining of meiotic cells was performed essentially as previously described by Hagan and Hyams (1988). To label the SPB, an affinity-purified rabbit polyclonal antibody against Sad1 (a generous gift from Drs. M. Shimanuki and O. Niwa, Kazusa DNA Research Institute, Kisarazu, Japan) was used (Hagan and Yanagida 1995). For viewing the localization of Taz1::GFP and Sad1 in the same meiotic cell, cells were grown at 19° for 3–4 days on MSA plates, fixed in 3.7% paraformaldehyde and 0.25% glutaraldehyde for 10 min, and stained with Sad1. The mouse monoclonal TAT1 antibody was used to stain microtubules (Woods *et al.* 1989). Secondary antibodies were fluorescein-conjugated donkey anti-rabbit antibody (Jackson Laboratories, West Grove, PA), Texas-red-conjugated goat anti-rabbit antibody (Jackson Laboratories), and fluorescein-conjugated rabbit anti-mouse antibody (Amersham Pharmacia Biotech, Braunschweig, Germany). To view green fluorescent protein (GFP)-tagged Taz1p and Pcp1p in fixed meiotic cells, cells were fixed in ice-cold 100% methanol for 10 min and then rehydrated sequentially in 75%, 50%, 25%, and 0% methanol in PBS, each for 5 min on ice. Cells were finally resuspended in PBS. To stain the nuclear DNA, 1 μg/ml DAPI was added to mounting solution (1 mg/ml ρ-phenylenediamine, 50% glycerol). Microscopic images were acquired with a Delta Vision System (Applied Precision) with an Olympus oil immersion objective lens (UPlan Apo 100×/NA 1.35). This system allows images to be taken under multiple wavelengths and with multiple Z optical sections. A stack of 18 Z-axis sections with a 0.2-μm interval was subjected to reiterative deconvolution (Chen *et al.* 1995). Final projections were obtained, processed using Priism (Chen *et al.* 1995) or SoftWoRx 2.50 (Applied Precision) and further edited with Adobe Photoshop 5.0 (Adobe).

**Microscopic observation of living cells for Swi6p::GFP and Taz1p::GFP:** *dot* mutants and wild-type homothallic strains carrying the integrated *swi6*$^+$*::GFP* and *taz1*$^+$*::GFP* fusion genes, respectively, were induced into mating and meiosis by streaking cells onto MSA plates or EMM2 plates. Zygotes were scraped off the plates 2–3 days later, suspended in SPA medium, and spotted onto a thin layer of 1% agarose on slides. Then cells were covered and spread by an 18 × 18-mm coverslip. Meiotic cells were examined under oil immersion lens as described above. Time-lapse images were collected with seven to nine Z-axis sections and 0.4-μm intervals between each section with an exposure time of 0.5 sec for Swi6::GFP and 0.8 sec for Taz1::GFP, over a 10-min period. Image stacks were acquired every 30–60 sec. Images for all time points were deconvolved, projected, and converted to either Quick Time Movie files or Tiff files by Priism (Chen *et al.* 1995) or SoftWoRx 2.50 programs on an SGI (Silicon Graphics) workstation for later study.

## RESULTS

**Screening for meiotic mutants affecting telomere clustering using Swi6::GFP:** To obtain a wide spectrum of fission yeast mutants affecting meiosis, we mutagenized yeast cultures and examined 20,000 colonies according to the method described by Uemura and Yanagida (1984; see materials and methods). We first screened for mutants that were defective in iodine staining. A total of 1200 white colonies, which did not show positive iodine staining, were obtained. From this collection, 76 strains were sporulation defective and displayed a variety of mutant phenotypes. By further examination of these mutant cells using DAPI, we were able to isolate 32 premeiotic and meiotic mutants. Complementation tests indicated that one of the mutants was allelic to *mat1-Pi* (Kelly *et al.* 1988) and two mutants were allelic to *mei2* (Bresch *et al.* 1968). These two genes are known to be important in meiosis.

We are particularly interested in studying telomere clustering in fission yeast during meiotic prophase. Thus, we transformed the above meiotic mutants with DNA fragments carrying the *swi6*$^+$::GFP fusion gene and examined the dynamic distribution pattern of Swi6::GFP. Swi6 is a heterochromatin-specific protein that binds to telomeres, centromeres, and the silent mating loci (Lorentz *et al.* 1994; Ekwall *et al.* 1995). Swi6::GFP has been used successfully in our lab to study chromosome segregation in mitotic mutants (Pidoux *et al.* 2000). As with vegetatively growing cells, low to medium levels of Swi6::GFP expression in meiotic cells are not toxic. *swi6*$^+$*::GFP*-transformed $h^{90}$ homozygous meiotic cells go through meiosis and sporulation without detectable differences from the untransformed wild-type $h^{90}$ homozygous meiotic cells. The nucleus is visible since the Swi6::GFP signal is also faintly diffuse within the nucleoplasm. In homothallic wild-type $h^{90}$ meiotic cells, the telomere Swi6::GFP signal appears as a single spot at the leading edge of conjugating haploid nuclei and of the fused horsetail zygotic nuclei (Figure 1B). Swi6::GFP foci positioned away from this leading edge within the body of the nucleus are presumably centromeres and silent mating loci. We followed the dynamic distribution pattern of Swi6::GFP in synchronized meiotic mutant cells during karyogamy or the horsetail stage. We judged the efficiency of telomere clustering by the following criteria: (1) if the telomere Swi6::GFP signal did not appear as a single spot but rather as multiple foci or as a diffuse, extended line at the leading edge of the nucleus, we scored telomere clustering as disrupted in this cell, and (2) since nuclear fusion and the horsetail movement are dynamic processes, disruption of telomere clustering should be observed at multiple time points during our 10-min observation period.

On the basis of these criteria, we found six mutants showing different patterns of defective telomere clustering as represented in Figure 1B. We named them *dot* mutants—*d*efective *o*rganization of *t*elomeres.

In mutant *dot-182* meiotic cells, telomere Swi6::GFP signals are typically seen as extended lines at the leading edge of the horsetail nuclei. In *dot-439* and *dot-143* mei-

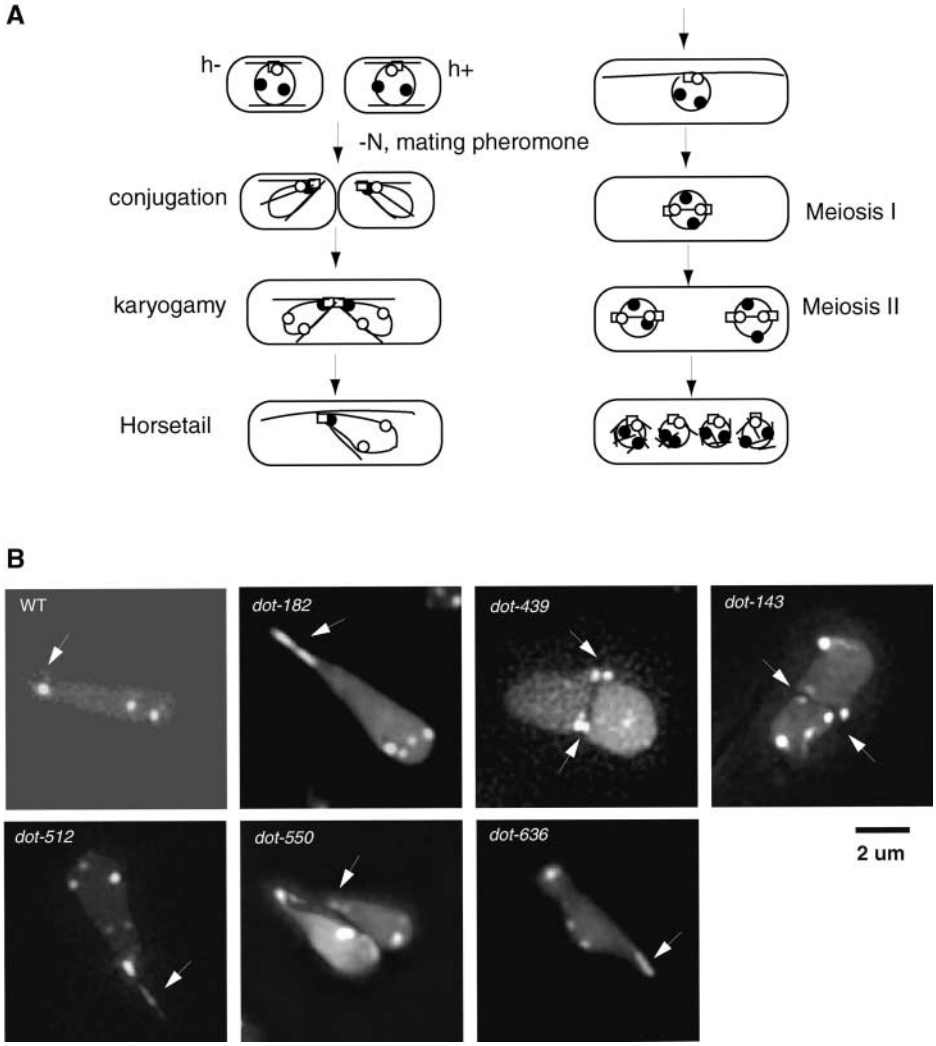


FIGURE 1.—(A) Nuclear architecture and microtubule reorganization during meiosis in fission yeast cells. Open squares, SPBs. Open circles, centromeres. Solid circles, telomere clusters. (B) Swi6::GFP distribution patterns during the karyogamy and horsetail stage in wild-type and *dot* cells. Each frame shows a single meiotic cell. In wild type, the telomere cluster is positioned at the leading edge of the horsetail nuclei as a single Swi6::GFP spot (indicated by arrowhead). The nucleus can be seen by the faint Swi6::GFP staining. In *dot-182*, telomere Swi6::GFP signals appeared as a stretched line. In *dot-439* and *dot-143*, two deformed haploid nuclei were trying to fuse at two sites, as seen by matched Swi6::GFP telomere signals (indicated by arrowheads). The normal shape of a conjugating haploid nucleus should be a teardrop-like shape with leading ends being pulled toward each other. In *dot-512*, *-550*, and *-636*, telomere signals are either stretched lines or distinct dots. *dot550* also shows twin horsetail nuclei.

otic cells during karyogamy, the two haploid nuclei appear to be contacting each other at two sites, matched by two telomere Swi6::GFP signals, instead of at a single site as in wild type (CHIKASHIGE *et al.* 1994). In *dot-550*, *-512*, and *-636* meiotic cells, telomere Swi6::GFP signals are spread out either as continuous stretched lines or as discrete, closely linked dots.

In addition to defective telomere clustering, observation of Swi6::GFP behavior also revealed other nuclear defects. In *dot-182*, the horsetail nuclei are often more elongated when compared to the wild type. In *dot-439* and *dot-143* cells, limited horsetail movement can be seen although nuclear fusion is defective. The typical teardrop shape of the nuclei is also lost in many cells. In *dot-550* cells, although the two haploid nuclei contact and seem to fuse at their tips, the nuclear fusion never proceeds beyond this point and the two unfused nuclei undergo their horsetail movement coordinately, exhibiting a twin horsetail phenotype. In many cases, this coordinate movement was disrupted by the final separation of the two nuclei. In *dot-512* and *-636*, horsetail movement is clumsy and lacks fluidity.

**Allelism of *dot* mutants:** All *dot* mutations are recessive. Thus to determine how many complementation groups are represented by *dot* mutants, heterothallic cells were mixed together and spotted on SPA plates to assess the occurrence of sporulation on the basis of iodine staining and microscope examination (see MATERIALS AND METHODS). All *dot* mutants complemented except for pairs between *dot-512*, *-550*, and *-636* (data not shown). To confirm the possible allelism existing among these mutants, heterozygous diploids of pairs among *dot-512*, *-550*, and *-636* were constructed. These diploid cells were stable and failed to undergo azygotic meiosis. Thus, the six mutants fall into four complementation groups with one group containing three alleles. These four groups were designated as *dot1*, *dot2*, *dot3*, and *dot4*. The specific alleles are *dot1-182*, *dot2-439*, *dot3-143*, *dot4-512*, *dot4-550*, and *dot4-636*.

Further genetic analyses, including complementation tests and linkage analyses, were performed to determine whether *dot* mutants are allelic to known mutants showing similar phenotypes. We first tested whether any of the *dot* mutants is allelic to *kms1*, a mutant of an SPB-

associated component showing defects in telomere clustering (Shimanuki *et al.* 1997). Heterothallic *dot* mutants were mated to a null allele of *kms1*, YJMB1261, and complementation was observed between them (data not shown). Thus, none of the *dot* genes is *kms1*$^+$. Next, we tested whether any of the *dot2-439*, *dot3-143*, and *dot4-550* mutants is allelic to *tht1*, a mutant defective in nuclear fusion that shows twin nuclei during the horsetail stage (Tange *et al.* 1998), because nuclear fusion is also defective in these *dot* mutants. Complementation was also found (data not shown). Since we used deletion alleles of *kms1*$^+$ and *tht1*$^+$, it is unlikely that the complementation between *dot* mutants and *kms1* is caused by intragenic complementation. We also transformed the *dot* mutants with plasmids bearing the *kms1*$^+$*::GFP* gene or the *tht1*$^+$ gene, and none of the *dot* mutants were rescued. The third gene tested for allelism with *dot* mutants was *sad1*$^+$, an essential gene encoding an SPB-associated protein (Hagan and Yanagida 1995) by linkage analyses. Homothallic *dot* mutants were mated with a heterothallic temperature-sensitive (ts) allele *sad1.1*. We screened at least 500 colonies by random spore analysis and did not find linkage between *sad1.1* and any of the *dot* mutants. The possible allelism between *taz1*, a mutant of a telomere component showing defective telomere clustering, and any of the *dot* mutants is also excluded since we can use the Taz1::GFP as a marker to show the defective telomere clustering in *dot* mutants without suppression or complementation of the mutant phenotypes.

Interestingly, when *h*$^{90}$*dot3-143* cells were crossed with *h*$^-$ and *h*$^+$ wild-type strains, we found that, although they can mate with both *h*$^-$ and *h*$^+$ cells, only *h*$^{90}$*dot3-143*/*h*$^-$ *dot3*$^+$ zygotic cells went through meiosis and formed asci, but *h*$^{90}$*dot3-143*/*h*$^+$ *dot3*$^+$ cells did not. This behavior of *h*$^{90}$*dot3-143* during meiosis suggested that *dot3* is an *h*$^-$-specific gene and may be related to the mating type locus. Therefore, we crossed *h*$^{90}$*dot3-143* with EG370, a strain carrying a mutation at *mat1-Mm*$^+$ (Egel and Gutz 1981). No complementation was observed on the basis of iodine staining and microscope examination. We also looked for linkage between *dot3-143* and *his2*$^-$, a marker tightly linked to *mat1-Mm*$^+$, by crossing *h*$^{90}$*dot3-143* with EG367 (*h*$^{90}$*Pm*$^-$*/M Pm*$^-$ *M his2 swi2-3 ade6-m210*). The genetic distance between *his2* and *mat1-Mm* is ~1 cM (Munz *et al.* 1989). We examined 159 *his*$^+$ spores from a cross between *h*$^{90}$*dot3-143* and EG367, and none of them showed recombination between *dot3-143* and *his2*. Since EG367 behaves as an *h*$^-$ strain and *h*$^{90}$*dot3-143* behaves as an *h*$^+$ strain, essentially all viable spores came from the interstrain mating but not from *h*$^{90}$ self-mating. Thus *dot3-143* is tightly linked with *his2* with a genetic distance of <2 cM. This is consistent with the observation that *dot3-143* is an allele of *mat1-Mm*. To prevent possible confusion in the future, we refer to *dot3-143* as *mat1-Mm143* from this point on.

*dot4* mutants are likely to be allelic to *mei4*$^+$, a gene encoding a meiotic transcription factor (Horie *et al.* 1998). All *dot4* mutants arrested in the horsetail stage, resembling the mutant phenotype of *mei4* (Olson *et al.* 1978). Thus, we constructed the heterozygous diploid of *mei4::ura4*$^+$ and *dot4-550* and found that the diploid cell failed to sporulate as revealed by iodine staining and microscopic examination. *dot4-512*, *-550*, and *-636* were renamed as *mei4-512*, *-550*, and *-636*.

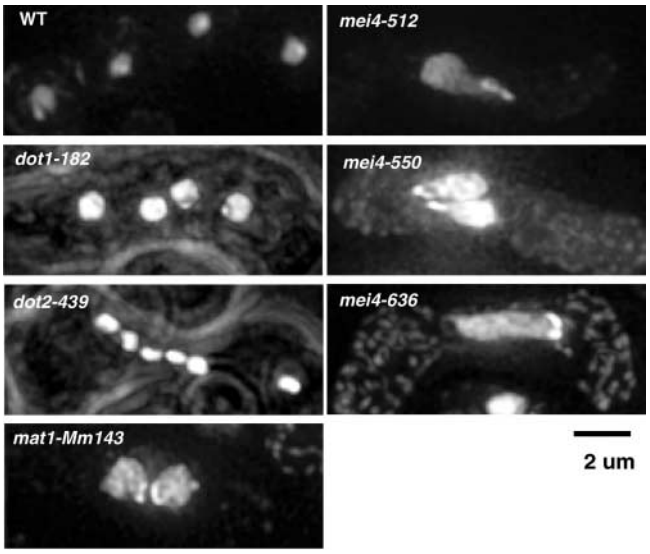


Figure 2.—Terminal phenotypes of *dot1* to *dot4* mutants during meiosis as shown by DAPI staining of cells 22 hr after mating. Each frame shows a single meiotic cell.

**Terminal phenotypes of *dot* mutants:** All *dot* mutants were originally identified by sporulation defects. To determine at which stage they arrested, *h*$^{90}$ *dot* cells were examined throughout meiosis. After 22 hr of nitrogen starvation, cells were collected, fixed with 2.5% glutaraldehyde, stained with DAPI, and examined under the microscope.

As shown in Figure 2, wild-type *h*$^{90}$ zygotic cells formed four spores and their nuclei were evenly spaced within an ascus. In the *dot1-182* mutant, most cells contained four daughter nuclei; however, the nuclei are often unevenly spaced. Also, the spore wall formation appeared to be severely impaired or delayed as we found very few spores from an *h*$^{90}$*dot1-182* × *h*$^{90}$*dot1-182* cross, plated on SPA medium for 3 days, even though some zygotes (10%) appear to have four normally sized and evenly spaced nuclei. The viable spore yield of *dot1-182* is ~$4.6 \times 10^{-5}$ spores/cell as shown in Table 2 (see materials and methods). *dot2-439* mutant meiotic cells typically have multiple micronuclei of varied sizes. Most *mat1-Mm143* meiotic cells arrest in the karyogamy stage with two haploid nuclei closely juxtaposed, but without undergoing nuclear fusion. Only 6% of zygotic cells complete meiosis and sporulate. The viable spore yield is also roughly estimated to be ~$2.4 \times 10^{-4}$ (Table 2). *mei4-512*, *-550*, and *-636* mutants are arrested at the horsetail stage, with only the *mei4-550* cells showing twin

**TABLE 2**

**Phenotypes of *dot* mutants at different stages of sexual development of *S. pombe***

| Strain | Karyogamy stage[a] | Horsetail stage[a] | Telomere clustering[b] | SPB integrity[b] | Meiosis I[c] | Meiosis II[c] | Sporulation[d] | Viable spore yield[e] |
|---|---|---|---|---|---|---|---|---|
| *dot1-182* | Normal | Defective movement | Defective | Disrupted | Normal | Defective | <1%, no microtubule bundles around nuclei | $4.6 \times 10^{-5}$ |
| *dot2-439* | No nuclear fusion | Limited movement | Defective | Disrupted | Defective spindle and Pcp1::GFP pattern | Defective spindle and Pcp1::GFP pattern | No | NA |
| *Mat1-Mm143* | No nuclear fusion; abnormal MT organization | Limited movement | Defective | Disrupted | NA[f] | NA | ~6% | $2.3 \times 10^{-4}$ |
| *mei4-512* | Normal | Limited movement | Defective | Disrupted | NA | NA | No | NA |
| *mei4-550* | No nuclear fusion | Twin horsetails; two MTOC[g] | Defective | Disrupted | NA | NA | No | NA |
| *mei4-636* | Normal | Limited movement | Defective | Disrupted | NA | NA | No | NA |

[a] Based on Swi6::GFP pattern and staining pattern of nuclei.
[b] Based on Taz1::GFP and Sad1 immunostaining during karyogamy and horsetail stages.
[c] Based on microtubule staining.
[d] Based on the percentage of zygotes showing asci. For wild type, the percentage is 90%.
[e] Calculated as the number of colonies from random spores plated on YES/number of vegetatively growing cells induced into meiosis. For wild type, it is 1.7 spores/cell.
[f] NA, not applicable.
[g] Microtubule organization center.

horsetail nuclei. These terminal meiotic phenotypes are consistent with our observations of the dynamic distribution pattern of Swi6::GFP in *dot* mutants. Table 2 summarizes the observed defects during meiosis in *dot* mutants.

**Defective telomere clustering in *dot* mutants:** One limitation of using Swi6::GFP as a marker for telomere clustering during meiotic prophase is that Swi6::GFP signals represent all the heterochromatin sites in the nucleus. To score telomere behavior, we focused our attention on regions around the tip of the nuclei where telomeres are normally located during meiotic prophase. However, in mutant cells in which telomere clustering is severely disrupted, such that telomeres are dispersed throughout the nucleus, we were unable to distinguish telomere Swi6::GFP signals from those of the centromeres and silent mating type loci. For the same reason, we could also miscount a Swi6::GFP centromere or silent mating locus signal as a telomere signal if it is near the leading edge of the nucleus.

To confirm our observations of defective telomere clustering in *dot* mutants and to evaluate the severity of these defects accurately, we examined the distribution of Taz1::GFP in both living cells and fixed meiotic cells, which were also stained with Sad1 antibody, a marker for the SPB (Hagan and Yanagida 1995). Fission yeast Taz1 is a homolog of Rap1 in budding yeast and specifically binds to telomeric sequences (Cooper *et al.* 1997). Figure 3A shows the distribution pattern of Taz1::GFP and Sad1 in wild-type and *dot* mutants during karyogamy or the horsetail stage. In wild-type $h^{90}$ cells, Taz1::GFP was visible as a single spot and colocalized with a single SPB Sad1 spot at the leading edge of the haploid nucleus during karyogamy and zygotic nucleus during the horsetail stage. This is consistent with the result obtained by fluorescence *in situ* hybridization (FISH) of premeiotic *S. pombe* cells using telomere-specific sequences (Chikashige *et al.* 1994). In *dot* mutants, multiple Taz1::GFP dots were seen in karyogamy or horsetail nuclei. In *dot1-182*, a large, brighter Taz1::GFP spot is seen at the leading edge of the horsetail nuclei immediately followed by a smaller and weaker Taz1:GFP spot. Both of them are colocalized with Sad1 foci. In *dot2-439*, two closely positioned haploid nuclei are undergoing the horsetail movement without complete fusion. However, the leading edges of two nuclei seem fused as indicated by a large, bright Taz1::GFP spot. Other smaller Taz1::

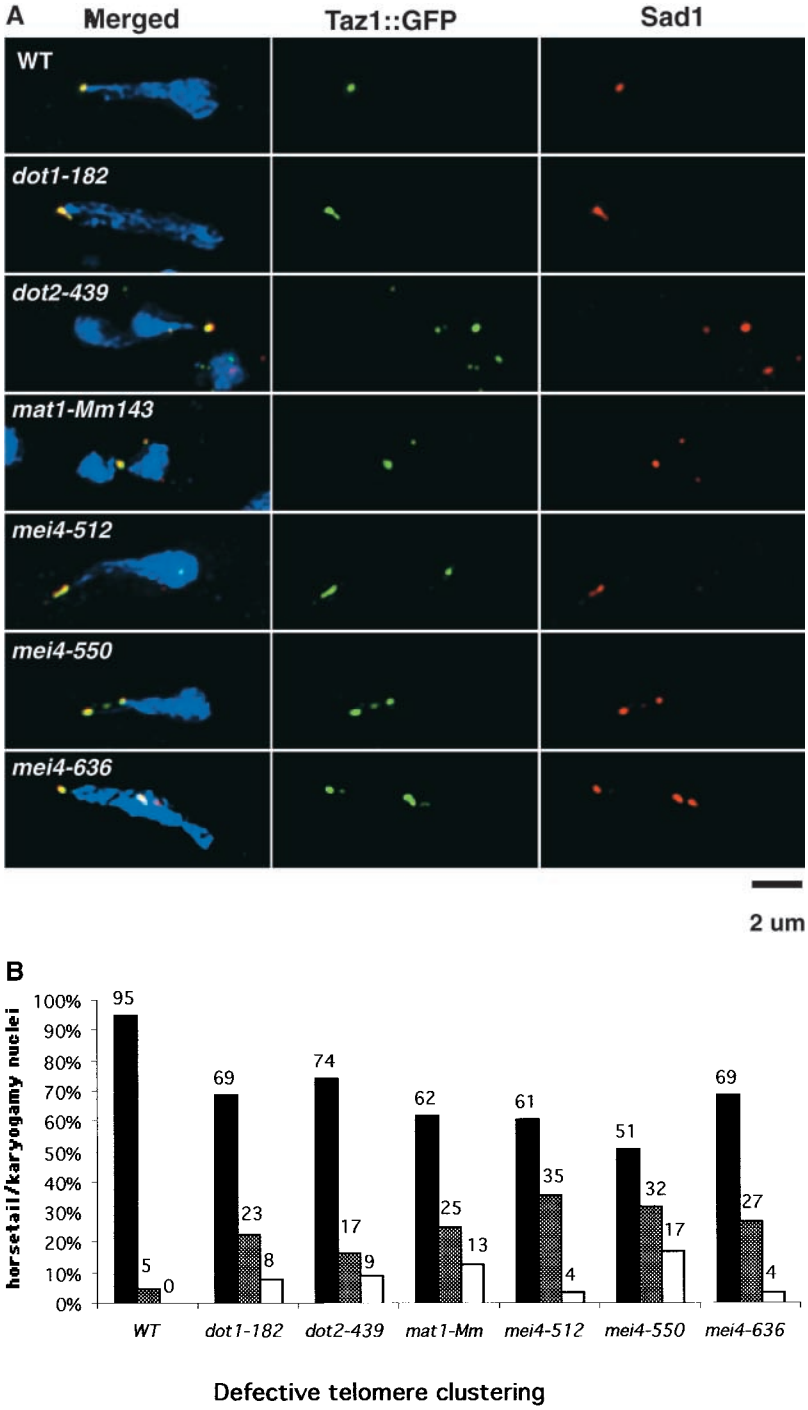


FIGURE 3.—Distribution pattern of Taz1::GFP and Sad1 in meiotic cells of WT and *dot* mutants during karyogamy or horsetail stages. (A) Triple-labeling of wild-type and *dot* meiotic cells. Pictures in the first column are merged from images of the second and third columns. Blue color represents DAPI staining of DNA. Green color represents Taz1::GFP labeling. Red color represents Sad1 staining. Yellow is the merged signal of the red and green. Green and blue signals are merged as the white. Each frame shows a single meiotic cell. The wild-type cell is in the horsetail stage. A single Taz1::GFP spot is colocalized with one Sad1 spot at the leading edging of the nucleus. In *dot* mutants, multiple Taz1::GFP foci are observed within nuclei. In many cells, these dispersed Taz1::GFP foci are colocalized with Sad1-staining foci. (B) Patterns of defective telomere clustering and their frequencies in *dot* mutants. Compared with $h^{90}$ cells, the frequency of multiple Taz1::GFP foci in *dot* meiotic cells was increased significantly. ■, One Taz1 dot at the leading edge of the nucleus; ▩, dispersed Taz1 dots near the leading edge of the nucleus; □, dispersed Taz1 dots far away from the leading edge of the nucleus. (C) Patterns of dispersed Sad1 nuclei staining and their frequencies in *dot* mutants. ■, One Sad1 dot at the leading edge of the nucleus; ▩, Sad1 dots near the leading edge of the nucleus; □, Sad1 dots far away from the leading edge of the nucleus. (D) A schematic illustration of the positional relationship between Taz1::GFP and Sad1 in wild-type and *dot* mutants. The frequency of each pattern is also shown. In the second, third, and fifth class, one mispositioned Taz1 or Sad1 spot may represent more than one Taz1 or Sad1 signal in *dot* cells.

GFP foci are seen behind the bright spot and within the nuclei. Two of the Taz1::GFP foci are colocalized with Sad1 foci. In *mat1-Mm143*, two haploid nuclei seem to be approaching each other. Their leading ends are fused, as shown by a single Taz1::GFP spot. In addition to the large Taz1::GFP signal at the leading edge, a smaller and weaker Taz1::GFP signal also can be seen in one of the haploid nuclei. Both Taz1::GFP signals are colocalized with Sad1 spots. In *mei4-512*, Taz1::GFP signals can also be seen as a short stretched line at the leading edge of the nucleus in addition to a weak spot. Another Taz1::GFP spot is located away from the leading edge of the nucleus. All the Taz1::GFP signals are colocalized with Sad1 except the one lagging behind the leading edge of the nucleus. In *mei4-550*, three Taz1::GFP foci are seen at the leading edge of the horsetail nuclei (another nucleus is behind the front nucleus and cannot be seen). All of them are colocalized with Sad1 signals. In *mei4-636*, two Taz1 foci, one larger and one smaller, are at the leading edge of the nucleus. The other three Taz1::GFP foci are located away from the leading edge. Most of the Taz1::GFP foci are colocalized wth Sad1 foci.

The frequencies of defective telomere clustering pat-

C

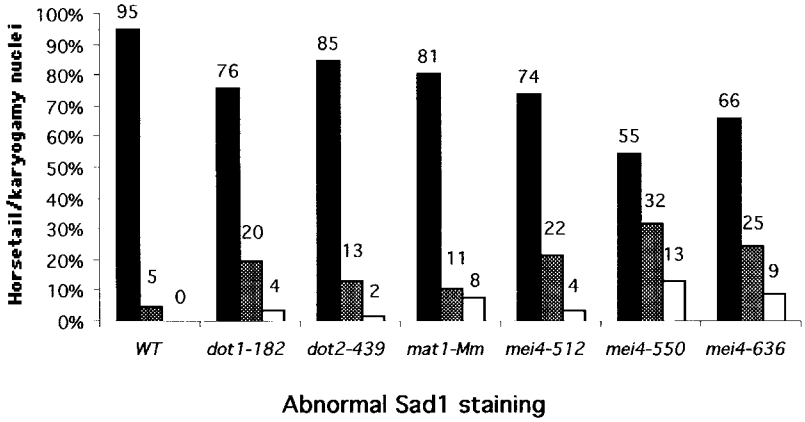


D

| ○ Sad1 ● Taz1 ● Sad1/Taz1 |  Class 1 |  Class 2 |  Class 3 |  Class 4 |  Class 5 |
|---|---|---|---|---|---|
| WT | 93% | 0% | 5% | 0% | 2% n=62 |
| *dot1-182* | 68% | 10% | 22% | 0% | 0% n=51 |
| *dot2-439* | 74% | 9% | 15% | 2% | 0% n=54 |
| *mat1-Mm143* | 57% | 21% | 6% | 11 % | 5% n=63 |
| *mei4-512* | 58% | 26% | 14% | 2% | 0% n=51 |
| *mei4-550* | 47 % | 6% | 28% | 15% | 4% n=53 |
| *mei4-636* | 62% | 4% | 27% | 7 % | 0% n=56 |

FIGURE 3.—*Continued.*

terns in *dot* mutants and in wild type are shown in Figure 3B. These patterns were classified according to the positioning of dispersed Taz1::GFP foci relative to the leading edge of the nucleus. The frequencies of aberrant patterns range from 26% in *dot2-439* to 49% in *mei4-550* and are significantly higher than the 5% in wild-type cells. We also noticed that most of the dispersed Taz1::GFP foci are located near the leading edge of the horsetail or karyogamy nuclei in *dot* mutants. These results confirmed our previous observations of defective telomere clustering in *dot* mutants using Swi6::GFP as a marker.

**Compromised SPB integrity in *dot* mutants:** In Figure 3A, abnormal Sad1 immunostaining patterns were also observed in *dot* cells in addition to dispersed Taz1::GFP foci. In wild-type cells, a single Sad1-immunostaining spot is found at the leading edge of the karyogamy or horsetail nucleus (Figure 3A). In contrast, in *dot* mutants, multiple Sad1 foci with varied intensities are observed within meiotic prophase nuclei as mentioned in the previous section. Patterns of aberrant Sad1 staining and their percentages in each *dot* mutant are described in Figure 3C. These frequencies range from 15% in *dot2-439* to 45% in *mei4-505*, while in wild-type cells only 5% of the cells show more than a single Sad1 spot. Interestingly, we found that many dispersed Taz1:: GFP signals in *dot* mutants were coincident with dispersed Sad1 foci (Figure 3A). The level of correlation between dispersed Taz1 and Sad1 signals varied according to the mutant. The positional relationships of Taz1 and Sad1 signals in *dot* mutants were categorized into five classes represented schematically in Figure 3D. The first class illustrates the normal wild-type positional relationship between Taz1 and Sad1. In the second class, dispersed Taz1 foci are not coincident with Sad1 foci. However, in the third class, dispersed Taz1 foci are completely colocalized with dispersed Sad1 foci. In the fourth class, while some dispersed Taz1 foci are seen

colocalized with Sad1 foci, the others are not. Cells of the fifth class show a normal single Taz1 spot, but multiple Sad1 foci.

The phenotype described above is similar to that reported for *kms1* mutants, which are also defective in telomere clustering. In the *kms1* mutant, multiple Sad1 immunostaining foci can be seen within the nucleus and some of them are colocalized with telomere signals (Shimanuki *et al.* 1997; Niwa *et al.* 2000) as indicated by FISH. Because Sad1 is an SPB-associated component throughout meiosis and is essential for mitosis (Hagan and Yanagida 1995), it has been used as a marker for monitoring the integrity of the SPB during meiosis (Shimanuki *et al.* 1997; Okazaki *et al.* 2000). Thus, as in the *kms1* mutant, we think the integrity of the SPB is also disrupted in *dot* mutants.

**Abnormal Pcp1::GFP distribution pattern in *dot2-439*:** To test whether *dot* mutants also have other SPB structural defects, we used Pcp1 as an additional marker for analyzing SPB integrity. Pcp1 is a homolog of Spc110 in fission yeast. It has been cloned recently by Trisha Davis' group and they were able to show that the Pcp1::GFP fusion protein localizes to the SPB as expected (M. Flory and T. Davis, personal communication). In budding yeast, Spc110 is an SPB central core component localized to the nuclear side of the central plaque (Rout and Kilmartin 1990; Sundberg *et al.* 1996) with its C-terminal domain interacting with calmodulin (Geiser *et al.* 1993) and its N-terminal domain interacting with Spc98, a component of the γ-tubulin complex (Knop and Schiebel 1997).

We examined the distribution pattern of Pcp1::GFP in living and fixed $h^{90}$ wild-type and *dot* mutants. The Pcp1::GFP signal during meiotic prophase, including the karyogamy and horsetail stages, was very weak in $h^{90}$ wild-type cells. By increasing exposure time to 4 sec, we were able to detect a single Pcp1::GFP spot at the leading edging of moving horsetail nuclei as expected (data not shown). After the horsetail stage and before entering to the first nuclear division, a bright Pcp1::GFP spot was found within the nucleus (Figure 4A). During meiosis II, two Pcp1::GFP spots were located next to each other or on opposite sides of the nucleus (Figure 4, B and C), presumably representing different stages of the second nuclear division. After meiosis II but before spore wall formation, each daughter nucleus had one Pcp1::GFP spot (Figure 4D). After spore wall formation, Pcp1::GFP signals were too weak to be detected. We did not observe any difference in Pcp1::GFP distribution pattern in *dot1-182*, *dot3-143*, and *dot4* mutants *vs.* wild-type cells. However, a striking difference between *dot2-439* and wild-type Pcp1::GFP distribution pattern during meiosis I and II was apparent, especially during the second meiotic division. The Pcp1::GFP signals in *dot2-439* during karyogamy and horsetail stage are hard to detect. Figure 4E shows that two approaching haploid nuclei in karyogamy have three Pcp1::GFP spots instead of one or two. Two of them are seen in a single haploid nucleus. In Figure 4F, the *dot2-439* zygotic nucleus has four Pcp1::GFP spots instead of two closely or oppositely positioned spots. Figure 4, G and H, shows two meiotic *dot2-439* cells in meiosis II. Both of them have Pcp1::GFP spots that appear disassociated from the nucleus. The second meiotic cell has in total six Pcp1::GFP spots with two spots in one nucleus, three spots in the second nucleus, and one spot in the cytoplasm between them. Figure 4I schematically illustrates the types of defects and their frequencies found in *dot2-439* cells during meiosis I and II. The left column under each category represents normal distributions of Pcp1::GFP, and the right column represents aberrant distribution patterns. As summarized in Figure 4, 57% of the *dot2-439* cells have an abnormal Pcp1::GFP pattern during meiosis. In wild-type cells, only 6% of the cells show similar phenotypes. Among the cells showing abnormal Pcp1::GFP distribution, 24% of them have Pcp1::GFP foci that are not associated with any nuclei.

**Microtubule organization in *dot* mutants during meiosis:** The SPB performs multiple functions during meiosis, including organization of cytoplasmic microtubules during meiotic prophase and spindle assembly in meiosis I and II. After cell fusion, the SPB is solely responsible for organizing cytoplasmic microtubules during meiotic prophase (Bähler *et al.* 1993; Svoboda *et al.* 1995; Ding *et al.* 1998; Hagan and Petersen 2000). If SPB integrity is compromised in any of the *dot* mutants, we might find some defects in microtubule organization during meiosis. Thus we studied the immunostaining pattern of microtubules in $h^{90}$ wild-type and *dot* mutant cells using TAT1 antibody, an anti-α-tubulin specific antibody (Woods *et al.* 1989). We found that *dot1*, *dot2*, *mat1-Mm143*, and *mei4-550* mutants have abnormal microtubule organization during meiosis.

The typical microtubule configurations in each stage of the sexual development for wild-type $h^{90}$ meiotic cells are shown in Figure 5, A–E, which includes karyogamy, the horsetail stage, meiosis I, meiosis II, and sporulation. These staining patterns are consistent with those previously reported (Bähler *et al.* 1993; Hagan and Yanagida 1995; Svoboda *et al.* 1995; Ding *et al.* 1998). *dot1-182* and *dot2-439* mutants have normal microtubule configurations early in meiosis during karyogamy and horsetail stages, but not in meiosis I and meiosis II stages. *dot1-182* shows defects in 25% of the meiotic cells during meiosis II (Figure 5, F–I). In Figure 5F, one nucleus in the zygote does not form a spindle; the other has an elongated spindle without chromosome segregation. In Figure 5G, both nuclei of the zygote have elongated spindles without accompanied chromosome segregation. In Figure 5H, both spindles appear to be monopolar spindles. Perhaps the most severe and prevalent defect in *dot1-182* is the absence of microtubule bundles around the nucleus after meiosis II and before spore wall formation (Figure 5I; compare with Figure

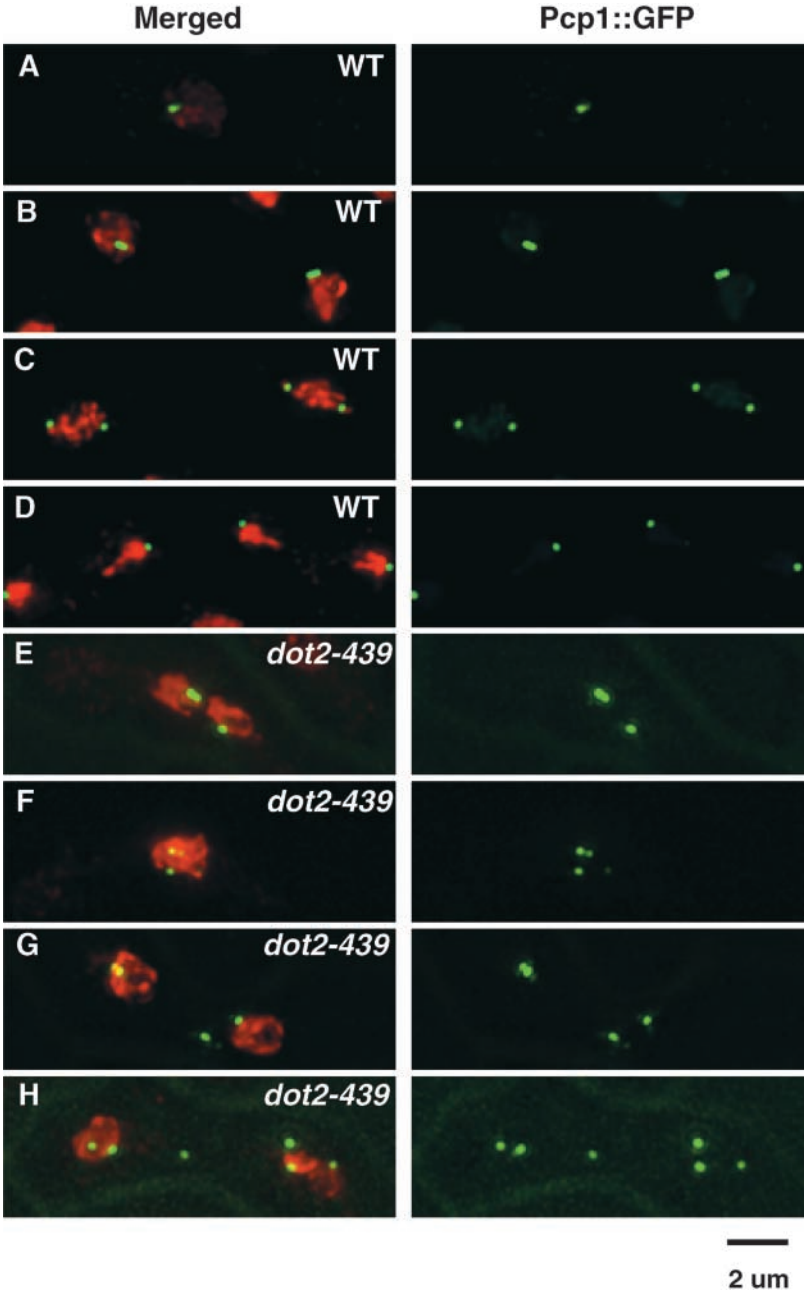


I

| | N | One nuclei | | Two nuclei | | Four nuclei | |
|---|---|---|---|---|---|---|---|
| WT | 85 | 35% | 0 | 27% | 1% | 32% | 1% |
| *dot2-439* | 142 | 8% | 9% | 28% | 32% | 7% | 9% |

FIGURE 4.—Pcp1::GFP (a central core component of the SPB) distribution pattern in wild-type $h^{90}$ (A–D) and *dot2-439* (E–H). Each frame shows a single meiotic cell. Green represents Pcp1::GFP and red represents DNA DAPI staining. (A) A zygotic nucleus just before meiosis I with a single Pcp1::GFP spot. (B) Two nuclei of a meiotic cell before entering into meiosis II. Each nucleus shows replicated but not separated SPBs. (C) Two nuclei of a meiotic cell in meiosis II. Each nucleus has two SPBs in opposite sides of the nucleus. (D) A meiotic cell shows four daughter nuclei after meiosis II before spore formation. Each nucleus has a bright Pcp1 spot. (E) Two haploid nuclei in a meiotic cell during the karyogamy stage have three Pcp1::GFP foci. (F) A zygotic nucleus just before meiosis I has four Pcp1::GFP foci. (G and H) Two nuclei of a meiotic cell in meiosis II with multiple Pcp1p::GFP foci. Some of the foci are not associated with any nuclei. Bar, 2 μm. (I) A schematic illustration of the distribution pattern of Pcp1::GFP in wild-type and *dot2-439* cells at different stages of the meiosis. Other abnormalities include aneuploid, nuclei without pcp1 staining wild type (WT), 4%; *dot2-439,* 7%. Solid circles represent Pcp1::GFP foci.

5E). Twenty-five percent of cells have spindle defects during meiosis I in *dot2-439*. Figure 5J shows a cell having an elongated spindle with no accompanied chromosome segregation and two extra microtubule staining sites within the condensed nucleus during meiosis I. Figure 5K shows another nucleus in meiosis I that fails to

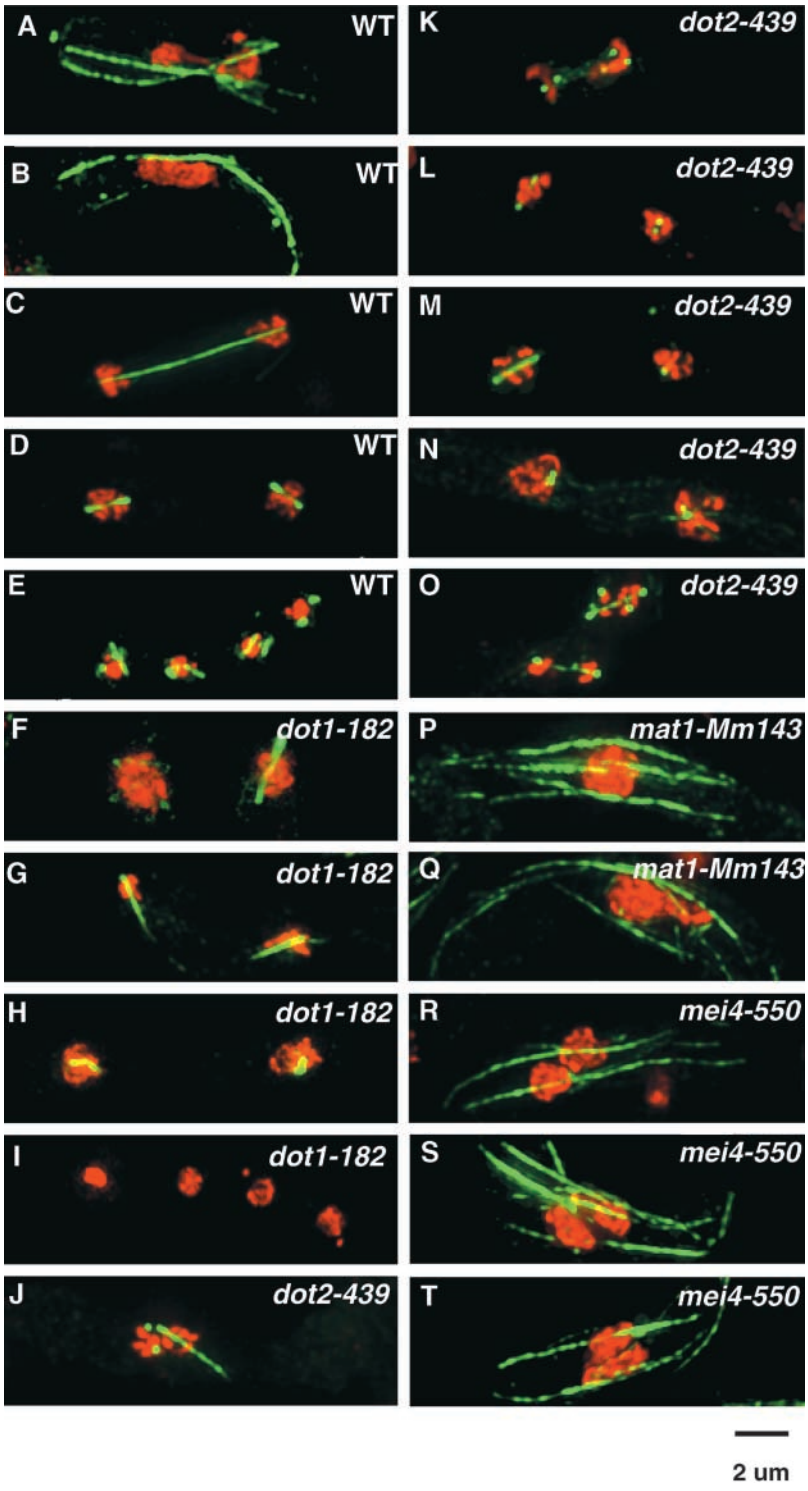


FIGURE 5.—MT organization during meiosis in wild-type $h^{90}$ (A–E) and *dot* mutants (F–T). Each frame shows one meiotic cell labeled with α-tublin antibody and DAPI. Microtubule staining is represented as green and DAPI staining is represented as red. A wild-type meiotic cell is shown in the karyogamy stage before nuclear fusion (A), in the horsetail stage (B), in meiosis I (C), in meiosis II (D), and in the sporulation stage (E). In the *dot1-182* mutant, 25% of cells in meiosis II have spindle defects as shown in F–H. The most typical and severe defect is the absence of microtubule bundles around the four daughter nuclei after meiosis II (I). In the *dot2-439* mutant, 25% of cells in meiosis I show spindle defects (J and K). More than 90% of cells show severe defects in spindle assembly in meiosis II (J–O). In *mat1-Mm143*, MTs seem to be organized from multiple MTOCs instead of from one (P) during the karyogamy stage. In *mei4-550*, more than two microtubule bundles are present during the horsetail stage (R–T) instead of one as in wild type (B). Bar, 2 μm.

form a normal spindle although multiple microtubule stainings can been seen. The most severe defects in *dot2-439* occur in meiosis II with >90% of the cells affected. Figure 5, L–O, shows several meiosis II defects observed in *dot2-439*, such as no spindle formation (L, M, right nuclei; N, left nucleus), a monopolar spindle (N, right nucleus), and a spindle with multiple poles (O, upper nucleus).

In *mat1-Mm143* meiotic cells that arrest in karyogamy, the most prevalent microtubule configuration we found is that shown in Figure 5P. Instead of the typical "X" microtubule array seen in wild-type $h^{90}$ cells during karyogamy (Figure 5A), multiple parallel microtubule arrays were seen around the nucleus, extending from one end of the cell to the other (Figure 5P). The presence of multiple microtubule organization center (MTOC) sites

is common during $G_2$ in wild-type vegetatively growing cells and in the final stage of meiosis preceding spore wall formation. In those *mat1-Mm143* cells that proceed into the horsetail stage without nuclear fusion, microtubule organizations remain abnormal (Figure 5Q) compared with those in wild-type cells (Figure 5B). Two *mei4* alleles, *mei4-512* and *mei4-636*, which were arrested in the horsetail stage, had microtubule configurations similar to that in wild-type cells (data not shown). However, *mei4-550* cells arrested at the horsetail stage frequently had multiple microtubule arrays, apparently nucleated from two independent MTOCs, as shown in Figure 5, R–T. These observations indicate that the MTOCs of the two haploid nuclei failed to fuse, remaining as microtubule nucleating centers.

## DISCUSSION

**Swi6::GFP is a sensitive marker for screening mutants affecting telomere clustering:** We have reported a screen that generated six meiotic mutants at four loci affecting telomere clustering during meiotic prophase. This is the first report of a systematic screen for mutants defective in telomere clustering from a group of meiotic mutants by observing the dynamic distribution pattern of a heterochromatin-binding protein—Swi6::GFP in fission yeast. There are several advantages for using Swi6::GFP to observe telomere clustering at the SPB. First, the stage of the cell in meiosis can be determined from the faint general nuclear staining by diffuse Swi6::GFP. Second, compared with weak Taz1::GFP signals, Swi6::GFP is much brighter, which allows quick, convenient screenings under low magnification using the epifluorescent light microscope. Third, the defects in chromosome end association near the leading edge of the horsetail nuclei may be more conspicuous not only because the Swi6::GFP signal is stronger than that of Taz1::GFP but also because Swi6::GFP binds to subtelomeric heterochromatin in addition to telomeres. This advantage is shown clearly in examining the phenotype of the *dot1-182* meiotic cells. Defective telomere clustering, as revealed by an extended line of Swi6::GFP signals, was found in almost every mutant cell examined (14 out of 14 living cells) during our 10-min observation period. However, in *dot1-182* mutant cells carrying the *taz1*$^+$*::GFP* gene, only ~50% of horsetail nuclei showed more than one telomere signal (8 out of 14 living cells). In these cells, generally, there were two or three closely positioned Taz1::GFP signals, with one being larger and brighter and the others smaller and fainter.

However, there are also disadvantages in using Swi6::GFP as a marker for monitoring chromosome end association. As mentioned previously, Swi6 is a heterochromatin-binding protein and binds to centromeres and the silent mating loci in addition to telomeres. Thus, it is possible that Swi6::GFP centromeres or the silent mating loci signals could be miscounted as telomere signals, especially in mutants that exhibit problems with centromere disassociation from SPB after conjugation. Therefore, first using Swi6::GFP and subsequently the Taz1::GFP provides a sensitive, quick, and accurate way to screen for mutants with defects in telomere clustering.

**Transcriptional factors are involved in telomere clustering:** Previous published studies have identified two kinds of proteins that affect telomere clustering in fission yeast during meiotic prophase. They are two telomere proteins, Taz1 and Lot2, and an SPB-associated protein, Kms1 (Shimanuki *et al.* 1997). A point mutation in γ-tubulin (Paluh *et al.* 2000) also disrupts telomere clustering as determined by Swi6p::GFP (J. Paluh and Z. Cande, personal communication).

This study indicates that transcriptional factors are also involved in telomere clustering and attachment. *dot3-143* is allelic to *mat1-Mm* and *dot4* mutants are allelic to *mei4*. *mat1-Mm*$^+$ and *mei4*$^+$ are two meiotic genes previously identified as encoding transcriptional factors, which play vital roles in regulating the progression of meiosis (Kelly *et al.* 1988; Aono *et al.* 1994; Horie *et al.* 1998) A mutant of *mat1-Mm*, B406, is blocked in $G_1$ before premeiotic DNA replication but after nuclear fusion (Egel and Egel-Mitani 1974). *mei4* mutants are arrested after DNA replication but before meiosis I. In *mei4* mutants, horsetail nuclei are accumulated (Olson *et al.* 1978; Horie *et al.* 1998; Hiraoka *et al.* 2000). The phenotype of defective telomere clustering has not been previously reported for mutants altered in these two genes. The terminal phenotype of *mat1-Mm143,* meiotic arrest at the karyogamy stage, is not observed in *mat1-Mm* (Shimoda *et al.* 1985). Therefore *mat1-Mm143* may represent a novel allele of this gene. *Mei4-550* is also likely to be a new allele of *mei4* because of the observed twin horsetail. Twin horsetail nuclei were previously reported only with *tht*$^+$, a gene involved in nuclear membrane fusion (Tange *et al.* 1998).

The involvement of meiotic-specific transcription factors in telomere clustering is surprising but not unreasonable. As master regulators of meiosis, they could affect the global reorganization of the nuclear architecture, which includes telomere clustering and attachment to the SPB, simply by the transcriptional regulation of proteins involved in this process. It will be part of our future work to determine the molecular nature of these mutations and, using microarray technology, to determine alteration of gene expression profiles in these mutants. For example, how are the transcription profiles of *mde*$^+$ genes changed in *dot4* mutants? *mde*$^+$ genes are transcriptionally dependent on *mei4*$^+$ (Abe and Shimoda 2000).

**The correlation of telomere clustering and SPB integrity:** The importance of the SPB in telomere clustering has been implied previously by the observation that telomeres cluster on the nuclear envelope adjacent to the SPB and is supported by the findings with the *kms1*$^+$ gene, which encodes an SPB protein. *kms1* mutants show

defective telomere clustering and fragmented SPBs during meiotic prophase as indicated by multiple Sad1-immunostaining dots within the nuclei (Shimanuki *et al.* 1997).

Our results are consistent with the idea that a link exists between telomere clustering and SPB integrity. All of the *dot* mutants isolated in this study also affect SPB integrity during meiotic prophase as shown by elevated frequency of multiple Sad1-immunostaining foci within nuclei. Many of these dispersed Taz1::GFP foci are colocalized with dispersed Sad1 foci. This coincidence in distribution suggests that the defective telomere clustering is correlated with impaired SPB integrity in *dot* mutants. The correlation is strong in *dot1-182*, *dot2-439*, *mei4-550*, and *mei4-636*, in which more than half of the cells defective in telomere clustering show complete colocalization of dispersed Taz1 spots with Sad1 foci, but it is less obvious in *mat1-Mm143* and *mei4-550*. In these two strains, less than half of the cells defective in telomere clustering show complete colocalization of dispersed Taz1 and Sad1 signals.

The colocalization of Sad1 and Taz1 signals in many cells of *dot* and *kms1* mutants also suggests a possible role for Sad1 as a linker between telomeres and the SPB. Sad1 and its *Caenorhabditis elegans* homolog, UNC84, have been proposed to link the nucleus to the SPB or the centrosome (Malone *et al.* 1999; Hagan and Petersen 2000) because of its putative transmembrane domain. In both organisms, the SPB or centrosome is on the cytoplasmic face of the nuclear envelope. In a recent study, Niwa *et al.* (2000) reported a direct interaction between Kms1 and Sad1. It will be interesting to determine whether the distribution pattern of Kms1 is altered in *dot* mutants.

Why are all *dot* mutants we identified also defective in SPB integrity? One possible explanation is that the *dot* mutants were isolated from a group of meiotic mutants defective in sporulation. A screen based on this severe defect may have confined us to a certain subset of telomere clustering mutants.

**Multiple malfunctions of SPB in *dot* mutants during meiosis:** The SPB has multiple functions during meiosis. These functions include microtubule organization, spindle assembly during meiosis I and II, and forespore membrane formation during sporulation. As shown in this article and previous studies, telomere clustering and attachment during karyogamy and the horsetail stage are also likely to be one of the SPB functions. How, then, does the SPB fulfill all those different functions?

One way is to use stage-specific SPB-associated components. The SPB is a dynamic protein complex with different constituents at each stage, and its makeup is both cell cycle and developmentally regulated. For example, Cut11, a protein essential for inserting the SPB into the nuclear envelope, is found on the SPB during nuclear division in meiosis I and II but not during the horsetail stage (West *et al.* 1998). SPB function also can be regulated by differentially modifying integral SPB components in each stage by an appropriate regulatory pathway. These two regulatory strategies are not incompatible and both could apply. Thus, mutations in integral components of the SPB or regulatory proteins, such as transcriptional factors, can affect multiple functions of the SPB in one stage, such as telomere clustering and microtubule organization during karyogamy in *mat1-Mm143*. These mutations can also affect SPB functions at different stages, such as telomere clustering during horsetail and spindle assembly during meiosis I and II in *dot2-439*.

*dot* mutants show multiple defects of SPB functions during meiosis in addition to telomere clustering. *dot1-182* cells show abnormal spindles in 25% of the cells during meiosis II and fail to form microtubule bundles or delay their formation around the nuclei after meiosis II. *dot2-439* cells show defects in spindle assembly during meiosis I and especially during meiosis II. *mat1-Mm143* and *mei4-550* cells have aberrant microtubule organization during karyogamy and horsetail stages. The extensive effects of *dot* mutants on several SPB functions during meiosis suggest that the $dot^+$ gene products are integral components of the SPB, which are associated with the SPB throughout meiosis, or that they are regulatory molecules modifying SPB function at a higher level. For example, mutants of transcription factors, such as *mat1-Mm143* and *mei4-512*, *-550*, and *-636*, affect SPB function by activation of expression of multiple meiotic-specific SPB components and its modifiers, which will be used in later stages of meiosis.

**Fragmented Pcp1 structure in *dot2-439* mutants:** A striking phenotype in one of the *dot* mutants, *dot2-439*, is the fragmented Pcp1 structure as revealed by multiple Pcp1::GFP foci during meiosis, especially at meiosis II. Multiple Spc110 foci within the nucleus were previously observed in vegetatively growing budding yeast cells by two research groups (Kilmartin and Goh 1996; Sundberg *et al.* 1996). Kilmartin and Goh found that overexpressed Spc110 and its truncated form, together with calmodulin, can form spheroidal polymers within the nucleus. Sundberg *et al.* (1996) also found that an Spc110 ts mutant that is defective in calmodulin binding showed similar intranuclear Spc110 bodies, which they referred to as intranuclear microtubule organization centers. In both cases, Spc110-containing bodies can nucleate microtubules and can even form small spindles with the SPB. Prompted by their results, we propose two possible reasons for the appearance of more than two Pcp1p foci within *dot2-439* meiotic cells. One is the inappropriate upregulation of expression of Pcp1 during meiosis so that excess Pcp1p self-aggregates and forms polymers within the nucleus. The dosage of SPB components is important in meiosis. Niwa's group recently reported a ubiquitin mutant that causes telomere detachment and declustering during meiotic prophase followed by chromosome missegregation (Okazaki *et al.* 2000). Thus, Dot2 may be a meiotic-specific regulatory

protein that controls the stoichiometry of the Pcp1 protein. A second explanation is that the *dot2*$^+$ gene encodes a Pcp1 interacting protein, such as calmodulin. The *dot2-439* mutation might weaken the interaction between calmodulin and Pcp1, resulting in the disassociation or failure of assembly of all Pcp1 into the SPB such that some Pcp1 self-aggregates. It is tempting to think that these Pcp1 bodies may also be able to nucleate microtubules, as they do in budding yeast, and even affect telomere attachment during meiotic prophase. We will pursue these possibilities in our future work. The future cloning and characterization of the *dot2*$^+$ gene will certainly provide important insights into SPB functions and the components required for telomere clustering.

We thank Drs. Julia P. Cooper, Trisha N. Davis, Keith Gull, and Osima Niwa for providing strains and antibodies. We are grateful to current members of the Cande lab for constructive discussions and comments on the manuscript, particularly Drs. Jan Paluh, Carrie Cowan, and Lisa Harper. This work is supported by grants from the National Institutes of Health (R01 GM23238, R01 GM48547) to W.Z.C.

## LITERATURE CITED

Abe, H., and C. Shimoda, 2000 Autoregulated expression of *Schizosaccharomyces pombe* meiosis-specific transcription factor Mei4 and a genome-wide search for its target genes. Genetics **154:** 1497–1508.

Alfa, C., P. Fantes, J. Hyams, M. Mcleod and E. Warbrik, 1993 *Experiments With Fission Yeast: A Laboratory Course Manual.* Cold Spring Harbor Laboratory Press, Cold Spring Harbor, NY.

Aono, T., H. Yanai, F. Miki, J. Davey and C. Shimoda, 1994 Mating pheromone-induced expression of the mat1-Pm gene of *Schizosaccharomyces pombe*: identification of signalling components and characterization of upstream controlling elements. Yeast **10:** 757–770.

Bähler, J., T. Wyler, J. Loidl and J. Kohli, 1993 Unusual nuclear structures in meiotic prophase of fission yeast: a cytological analysis. J. Cell Biol. **121:** 241–256.

Bass, H. W., W. F. Marshall, J. W. Sedat, D. A. Agard and W. Z. Cande, 1997 Telomeres cluster de novo before the initiation of synapsis: a three-dimensional spatial analysis of telomere positions before and during meiotic prophase. J. Cell Biol. **137:** 5–18.

Bresch, C., G. Müller and R. Egel, 1968 Genes involved in meiosis and sporulation of a yeast. Mol. Gen. Genet. **102:** 301–306.

Chen, H., J. R. Swedlow, M. Grote, J. W. Sedat and D. A. Agard, 1995 The collection, processing, and display of digital three-dimensional images of biological specimens, pp. 197–210 in *Handbook of Biological Confocal Microscopy*, edited by J. B. Pawley. Plenum Press, New York.

Chikashige, Y., D.-Q. Ding, H. Funabiki, T. Haraguchi and S. Mashiko, 1994 Telomere-led premeiotic chromosome movement in fission yeast. Science **264:** 270–273.

Chikashige, Y., D.-Q. Ding, Y. Imai, M. Yamamoto, T. Haraguchi *et al.*, 1997 Meiotic nuclear reorganization: switching the position of centromeres and telomeres in fission yeast *Schizosaccharomyces pombe*. EMBO J. **16:** 193–202.

Cooper, J. P., E. R. Nimmo, R. C. Allshire and T. R. Cech, 1997 Regulation of telomere length and function by a Myb-domain protein in fission yeast. Nature **385:** 744–747.

Cooper, J. P., U. Watanabe and P. Nurse, 1998 Fission yeast Taz1 protein is required for meiotic telomere clustering and recombination. Nature **392:** 828–831.

Dernburg, A. F., J. W. Sedat, W. Z. Cande and H. Bass, 1995 Cytology of telomeres, pp. 295–338 in *Telomeres*, edited by E. H. Blackburn and C. W. Greider. Cold Spring Harbor Laboratory Press, Cold Spring Harbor, NY.

Ding, D.-Q., Y. Chikashige, T. Haraguchi and Y. Hiraoka, 1998 Oscillatory nuclear movement in fission yeast is driven by astral microtubules, as revealed by continuous observation of chromosomes and microtubules in living cells. J. Cell Sci. **111:** 701–712.

Egel, R. and M. Egel-Mitani, 1974 Pre-meiotic DNA synthesis in the fission yeast. Exp. Cell Res. **88:** 127–134.

Egel, R., and H. Gutz, 1981 Gene activation by copy transposition in mating-type switching of a homothallic fission yeast. Curr. Genet. **3:** 5–12.

Egel, R., M. Willer, S. Kjaerulff, J. Davey and O. Nielsen, 1994 Assessment of pheromone production and response in fission yeast by a halo test of induced sporulation. Yeast **10:** 1347–1354.

Ekwall, K., J. P. Javerzat, A. Lorentz, H. Schmidt, G. Cranston *et al.*, 1995 The chromodomain protein Swi6: a key component at fission yeast centromeres. Science **269:** 1429–1431.

Gutz, H., H. Heslot, U. Leupold and N. Loprieno, 1974 *Schizosaccharomyces pombe*, pp. 395–446 in *Handbook of Genetics*, edited by R. C. King. Plenum Press, New York.

Hagan, I., and J. S. Hyams, 1988 The use of cell division cycle mutants to investigate the control of microtubule distribution in the fission yeast *Schizosaccharomyces pombe*. J. Cell Sci. **89:** 343–357.

Hagan, I., and J. Petersen, 2000 The microtubule organizing centers of *Schizosaccharomyces pombe*. Curr. Top. Dev. Biol. **49:** 133–159.

Hagan, I., and M. Yanagida, 1995 The product of the spindle formation gene sad1 associates with the fission yeast *Schizosaccharomyces pombe*. J. Cell Biol. **129:** 1033–1047.

Hiraoka, Y., D. Ding, A. Yamamoto, C. Tsutsumi and Y. Chikashige, 2000 Characterization of fission yeast meiotic mutants based on live observation of meiotic prophase nuclear movement. Chromosoma **109:** 103–109.

Horie, S., Y. Watanabe, K. Tanaka, S. Nishiwaki, H. Fujioka *et al.*, 1998 The *Schizosaccharomyces pombe mei4*$^+$ gene encodes a meiosis-specific transcriptional factor containing a forkhead DNA-binding domain. Mol. Cell. Biol. **18:** 2118–2129.

John, B., 1990 *Meiosis.* Cambridge University Press, New York.

Kelly, M., J. Burke, M. Smith, A. Klar and D. Beach, 1988 Four mating-type genes control sexual differentiation in the fission yeast. EMBO J. **7:** 1537–1547.

Knop, M., and E. Schiebel, 1997 Spc98p and Spc97p of the yeast γ-tublin complex mediate binding to the spindle pole body via their interaction with Spc110p. EMBO J. **16:** 6985–6995.

Kilmartin, J. V., and P.-Y. Goh, 1996 Spc110p: assembly properties and role in the connection of nuclear microtubules to the yeast spindle pole body. EMBO J. **15:** 4592–4602.

Loidl, J., 1990 The initiation of meiotic chromosome pairing: the cytological view. Genome **33:** 759–778.

Lorentz, A., K. Osterman, O. Fleck and H. Schmidt, 1994 Switching gene swi6, involved in repression of silent mating type loci in fission yeast, encodes a homologue of chromatin-associated proteins from *Drosophila* and mammals. Gene **143:** 139–143.

Malone, C. J., W. D. Fixsen, H. R. Horvitz and M. Han, 1999 UNC-84 localizes to the nuclear envelope and is required for nuclear migration and anchoring during *C. elegans* development. Development **126:** 3171–3181.

Moreno, S., A. Klar and P. Nurse, 1991 Molecular genetic analysis of the fission yeast *Schizosaccharomyces pombe*. Methods Enzymol. **194:** 795–823.

Munz, P., K. Wolf, J. Kohli and U. Leupold, 1989 Genetics overview, pp. 1–30 in *Molecular Biology of the Fission Yeast*, edited by A. Nasim, P. Young and B. Johnson. Academic Press, London.

Nimmo, E. R., A. L. Pidoux, P. E. Perry and R. C. Allshire, 1998 Defective meiosis in telomere-silencing mutants of *Schizosaccharomyces pombe*. Nature **392:** 825–828.

Niwa, O., M. Shimanuki and F. Miki, 2000 Telomere-led bouquet formation facilitates homologous chromosome pairing and restricts ectopic interaction in fission yeast meiosis. EMBO J. **19:** 3831–3840.

Okazaki, K., H. Okayama and O. Niwa, 2000 The polyubiquitin gene is essential for meiosis in fission yeast. Exp. Cell Res. **254:** 143–152.

Olson, L. W., U. Eden, M. Egel-Mitani and R. Egel, 1978 Asynaptic meiosis in fission yeast? Hereditas **89:** 189–199.

Paluh, J. L., E. Nogales, B. R. Oakley, K. McDonald, A. L. Pidoux *et al.*, 2000 A mutation in γ-tubulin alters microtubule dynamics

and organization and is synthetically lethal with the kinesin-like protein Pkl1p. Mol. Biol. Cell **11:** 1225–1239.

Pidoux, A. L., S. Uzawa, P. Perry, W. Z. Cande and R. C. Allshire, 2000 Live analysis of lagging chromosome behavior during anaphase and their effect on spindle elongation rate in fission yeast. J. Cell Sci. **113:** 4177–4191.

Robinow, C. F., 1977 The number of chromosomes in *Schizosaccharomyces pombe*: light microscopy of stained preparations. Genetics **87:** 491–497.

Robinow, C. F., and J. S. Hyams, 1989 General cytology of fission yeast, pp. 273–330 in *Molecular Biology of the Fission Yeast*, edited by A. Nasim, P. Young and B. Johnson. Academic Press, San Diego.

Rout, M. P., and J. V. Kilmartin, 1990 Components of the yeast spindle and spindle pole body. J. Cell Biol. **111:** 1913–1927.

Scherthan, H., J. Bahler and J. Kohli, 1994 Dynamics of chromosome organization and pairing during meiotic prophase in fission yeast. J. Cell Biol. **127:** 273–285.

Shimanuki, M., F. Miki, D.-Q. Ding, Y. Chikashige and Y. Hiraoka, 1997 A novel fission yeast gene, *kms1*$^+$, is required for the formation of meiotic prophase-specific nuclear architecture. Mol. Gen. Genet. **254:** 238–249.

Shimoda, C., A. Hirata, M. Kishida, T. Hashida and K. Tanaka, 1985 Characterization of meiosis-deficient mutants by electron microscopy and mapping of four essential genes in the fission yeast *Schizosaccharomyces pombe*. Mol. Gen. Genet. **200:** 252–257.

Sundberg, H. A., L. Goetsch, B. Byers and T. N. Davis, 1996 Role of calmodulin and Spc110p interaction in the proper assembly of spindle pole body components. J. Cell Biol. **133:** 111–124.

Svoboda, A., J. Baehler and J. Kohli, 1995 Microtubule-driven nuclear movements and linear elements as meiosis-specific characteristics of the fission yeasts *Schizosaccharomyces versatilis* and *Schizosaccharomyces pombe*. Chromosoma **104:** 203–214.

Tange, Y., T. Horio, M. Shimanuki, D.-Q. Ding and Y. Hiraoka, 1998 A novel fission yeast gene, *tht1*$^+$, is required for the fusion of nuclear envelopes during karyogamy. J. Cell Biol. **140:** 247–258.

Trelles-Sticken, E., M. E. Dresser and H. Scherthan, 2000 Meiotic telomere protein Ndj1p is required for meiosis-specific telomere distribution, bouquet formation and efficient homologue pairing. J. Cell Biol. **151:** 95–106.

Uemura, T., and M. Yanagida, 1984 Isolation of type I and II DNA topoisomerase mutants from fission yeast: single and double mutants show different phenotypes in cell growth and chromatin organization. EMBO J. **3:** 1737–1744.

West, R. R., E. V. Vaisberg, R. Ding, P. Nurse and J. R. McIntosh, 1998 *Cut11*$^+$: a gene required for cell cycle-dependent spindle pole body anchoring in the nuclear envelope and bipolar spindle formation in *Schizosaccharomyces pombe*. Mol. Biol. Cell **9:** 2839–2855.

Woods, A., T. Sherwin and R. Sasse, 1989 Definition of individual components within the cytoskeleton of *Trypanosoma brucei* by a library of monoclonal antibodies. J. Cell Sci. **93:** 491–500.

Yamamoto, A., R. R. West, J. R. McIntosh and Y. Hiraoka, 1999 A cytoplasmic dynein heavy chain is required for oscillatory nuclear movement of meiotic prophase and efficient meiotic recombination in fission yeast. J. Cell Biol. **145:** 1233–1249.

Zickler, D., and N. Kleckner, 1998 The leptotene-zygotene transition of meiosis. Annu. Rev. Genet. **32:** 619–697.

Communicating editor: G. R. Smith